Reliability Improvement of Stern Tube Bearing Considering Propeller Shaft Forces during Ship Turning

RYOTA KUROIWA*1 AKIRA OSHIMA*1
TADASUKE NISHIOKA*1 TOMOHIRO TATEISHI*2
KENJI OHYAMA*2 TAKASHI ISHIJIMA*2

To respond to the recent increase in container transportation and the pursuit of higher economic efficiency of ocean transportation, container ships are getting bigger and have higher propulsive power. Due to the increased propulsive power and propeller thrust, the propeller weights and the propeller shaft forces of these ships have become larger than those of past ones. Also the risk of uneven contact and seizure of the stern tube bearings is increasing. Therefore, the stern tube bearing design has become very important. By considering not only propeller weights but also propeller shaft forces for the stern tube bearing designs, Mitsubishi Heavy Industries, Ltd. (MHI) offers ships that are free from bearing problems.

1. Introduction

Stern tube bearing problems forces a ship out of service until the bearing is repaired. Considering the huge losses during this period of inactivity the reliability of the stern tube bearing is extremely important. MHI therefore designs stern tube bearings while considering, in addition to the propeller weight, the forces technically termed propeller shaft forces(1) (to be introduced in detail in Section 3 of this report).

To verify this design method, we conducted model tests to measure the propeller shaft forces(2) and measured the oil film thickness inside a stern tube bearing in a sea trial. The results from these have confirmed that the design method is effective.

This report introduces our practice for designing stern tube bearings. In addition, it also discusses a prediction method for propeller shaft forces that uses CFD and manoeuvring simulation.

2. Design procedure for stern tube bearings

At the stern, as shown in **Fig. 1**, a ship has a pipe-like structure called a stern tube, through which runs a propeller shaft. The stern tube also houses a stern tube bearing(3). MHI follows the procedure shown in **Fig. 2** when designing stern tube bearings. The following paragraphs outline this design procedure.

Studying the stern tube bearing dimensions and the bearing profile shown in **Fig. 3** takes place at an early stage of the ship design. Since neither the hull form of the ship nor the propeller geometry have been fixed yet, the study is carried out by using the hull form and the propeller of an earlier plan.

When designing the bearing dimensions and profile, an elastic beam calculation (static alignment calculation) is carried out considering only the propeller weight while assuming that the ship is still. The specific load on the stern tube bearing and the bending stress of shaft are designed under the criteria of the Classification Society standards.

However, with ships getting bigger and bigger, propeller shaft forces have reached almost the same level as propeller weight. Thus, to tentatively determine the bearing dimensions and profile, we also carry out a dynamic alignment calculation, in addition to the propeller weight, the propeller shaft forces generated when for example the ship turns.

A robust design called the Taguchi Method (see note) is also used to design the bearing profile.

With the design developing further and after deciding the ship specifications and the propeller profile, the static alignment calculation and the dynamic alignment calculation are performed again using this final propeller geometry to confirm the stern tube bearing performance. At this stage, if the results comply with the standards established by the Classification Society and secure a sufficient lubrication film thickness, the bearing dimensions and its profile become final.

Note: The method of developing products is based on statistics so that a product's functions deteriorate as little as possible even when the product is subject to the effects of external disturbances such as variations in the constituent parts or materials, inconsistent production processes, variations in the operating environment or the internal degradation of a product that can cause product failure or functional degradation.

*1 Nagasaki Research & Development Center, Technical Headquarters
*2 Nagasaki Shipyard & Machinery Works

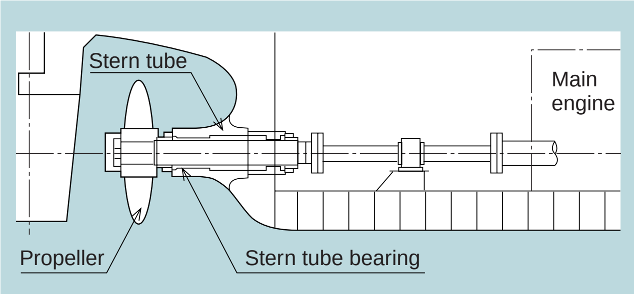

Fig. 1 Shaft arrangement
The stern tube houses two bearing bushes at its ends. The one at the rear, AFT bush, is called the stern tube bearing in this report.

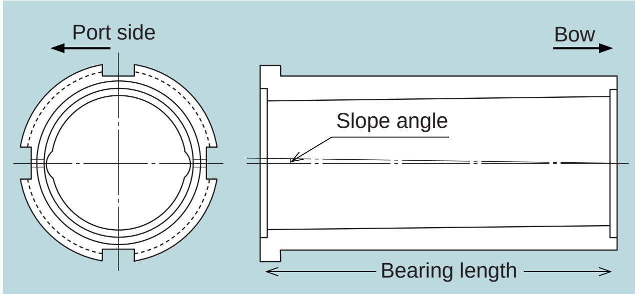

Fig. 3 Stern tube bearing profile
The dynamic alignment calculation helps determine the length and slope angle of the bearing.

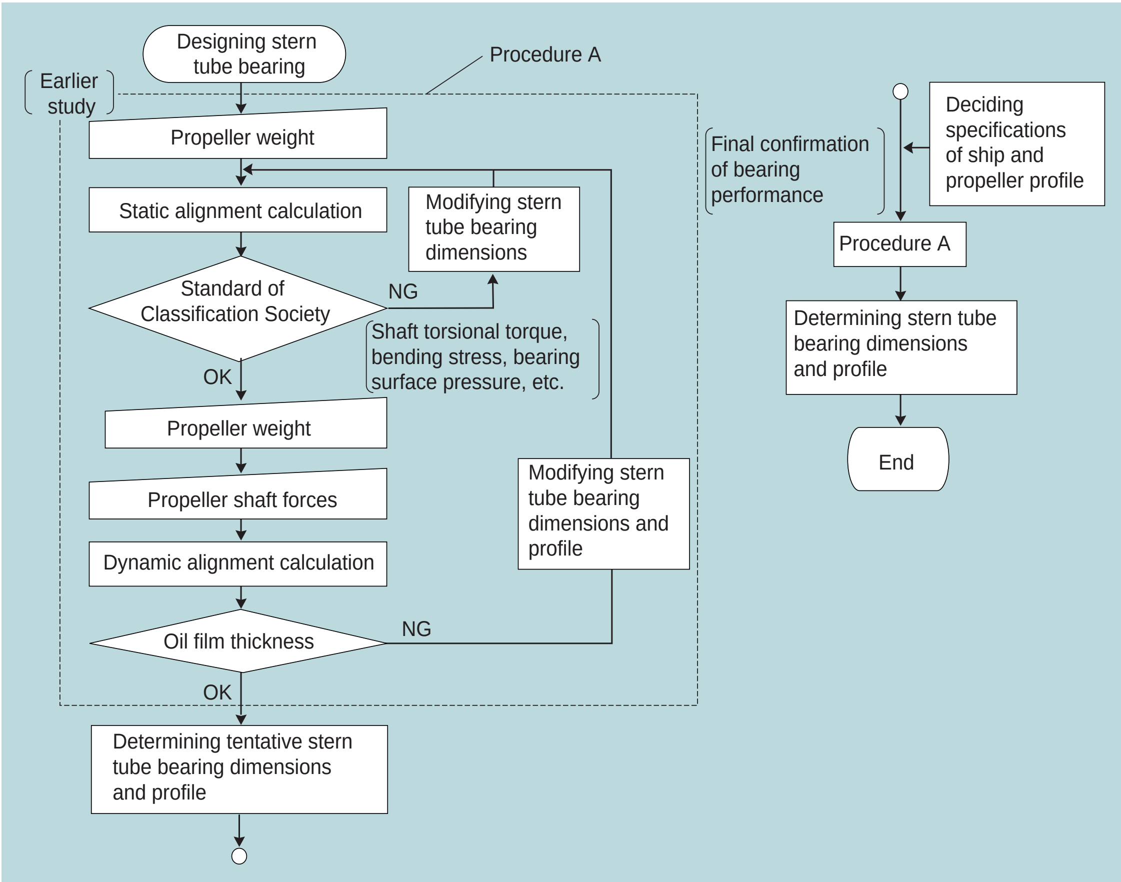

Fig. 2 Procedure for designing stern tube bearing
Stern tube bearings are designed by static and dynamic alignment calculations.

3. Propeller shaft forces

This section explains the propeller shaft forces that appear often in this report.

A screw propeller profile rotates symmetrically with respect to the propeller shaft. The propeller generates only thrust and torque if it operates in a uniform flow in the direction of the circumference. In reality, however, since it operates in a non-uniform flow at the rear of a hull, it generates forces and moments besides the thrust and torque. These forces and moments are collectively termed propeller shaft forces.

With the propeller co-ordinate system defined as shown in **Fig. 4**, the elements affecting the stern tube bearing design are the horizontal and vertical forces Fy and Fz and the vertical and horizontal bending moments My and Mz. Here, My and Mz are generated because the thrust is not uniform in the tangential direction while Fy and Fz are generated because the forces generating torque are not uniform in the tangential direction.

Generally, ships operate in various modes including running straight, turning and crabbing. Of these, a significantly strong lateral flow acts at the propeller position when the ship is turning at its maximum rudder angle. This causes the propeller shaft forces to increase to equal the propeller weight, making the stern tube bearing face the heaviest loads.

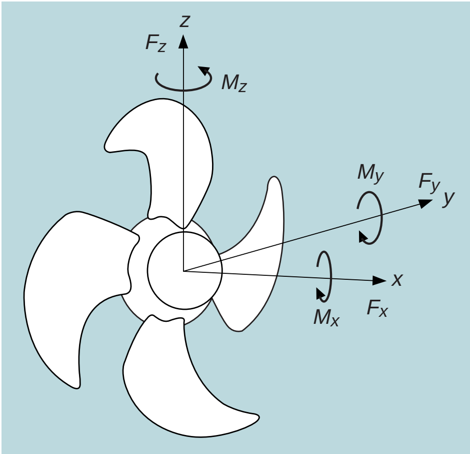

Fig. 4 Propeller co-ordinate system
Fx, *Fy* and *Fz* are defined as forces acting in the directions of the x, y and z axes, respectively. *Mx*, *My* and *Mz* are defined as moments of force with respect to the corresponding axes.

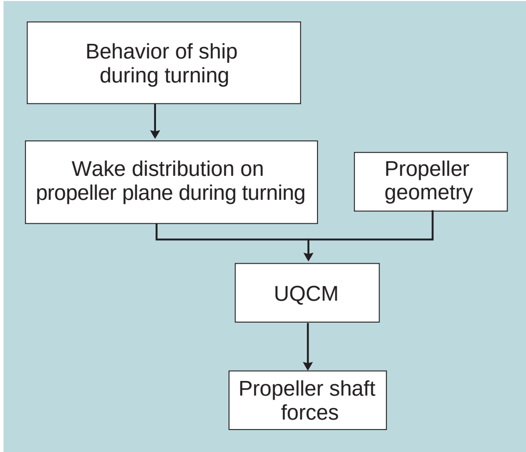

Fig. 5 Procedure for estimating propeller shaft forces
The ship behavior when turning is estimated to obtain the wake distribution on the propeller under these conditions. Given the wake distribution and the propeller profile, UQCM calculates the propeller shaft forces.

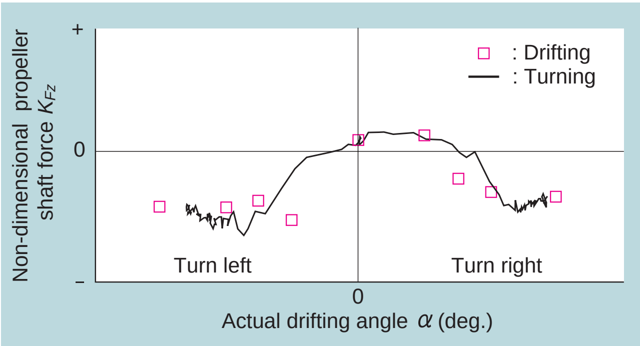

Fig. 6 Propeller shaft forces during turning and drifting
The figure shows K_{Fz} as a representative value. The propeller shaft forces both during turning and during drifting agree well.

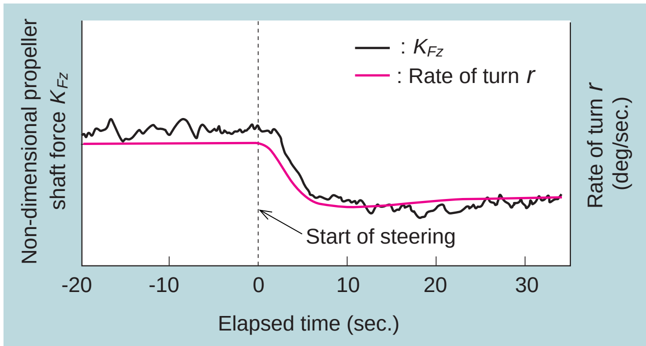

Fig. 7 Changes in propeller shaft forces during turning
The figure shows K_{Fz} as a representative value. The propeller shaft forces change nearly in proportion to the changes in the rate of turn *r*.

4. Method of estimating propeller shaft forces

4.1 Procedure for estimating propeller shaft forces

Figure 5 shows the procedure for estimating the propeller shaft forces. First, we estimate the motion characteristics of the ship when turning to obtain the actual drifting angle, which we will discuss below. Then, we estimate the wake distribution on the propeller plane at the actual drifting angle. Finally, we input the resulting wake distribution on the propeller plane and the propeller geometry to UQCM[(4)] (unsteady quasi-continuous method: an MHI developed method of calculating the propeller characteristics based on the unsteady lifting surface theory) and calculate the non-dimensional values of propeller shaft forces K_{Fy}, K_{Fz}, K_{My} and K_{Mz} as shown in Equation (1).

$$K_{Fy}=\frac{F_y}{\rho n^2 D^4},\quad K_{Fz}=\frac{F_z}{\rho n^2 D^4}$$
$$K_{My}=\frac{M_y}{\rho n^2 D^5},\quad K_{Mz}=\frac{M_z}{\rho n^2 D^5} \qquad (1)$$

Where, ρ is the density of sea water, n is the propeller rotation speed, and D is the propeller diameter.

To estimate the propeller shaft forces while the ship is turning it is necessary to know the wake distribution on the propeller plane under these conditions. However, since it is extremely difficult to obtain the wake distribution through model tests or numerical calculations, the wake distribution in a drifting condition that has an equivalent flow towards the propeller plane is substituted. In **Fig. 6** two kinds of non-dimensional propeller shaft forces are compared. One type is the measurement results from a turning test and the other is the calculated results using the wake distribution in a drifting condition. The two agree well, so it is reasonable to substitute the drift wake distribution.

4.2 Estimating actual drifting angles

When a ship starts to turn, the rate of turn *r* increases rapidly. This causes a significantly strong lateral flow to be generated. The rate of turn reaches its peak value immediately after starting to turn and before it falls to a steady state. As shown in **Fig. 7**, the propeller shaft forces (non-dimensional values) change nearly in proportion to the changes in the rate of turn and reach an approximate maximum when the rate of turn is at the maximum. The maximum propeller shaft forces are maintained even after enough time has elapsed for the ship to have reached steady-state turning. Thus, steady-state turning causes huge propeller shaft forces to act on the stern tube bearing for a long time, putting the bearing under a severe load. Therefore, the stern tube bearing design takes into account the propeller shaft forces generated in steady-state turning.

During turning, as shown in **Fig. 8**, the flow against the propeller plane is at angle α which is derived from the drifting angle β and the rate of turn. The angle is termed the actual drifting angle and is calculated by Equation (2).

$$\alpha = \beta + tan^{-1}\left(\frac{x_p}{U}\cdot r\right) \doteqdot \beta + \frac{x_p}{U}\cdot r \qquad (2)$$

where, xp is the distance from the propeller to the gravitational center of the hull, and U is the velocity of the ship.

By using a manoeuvring simulation we can obtain the actual drifting angle for each individual ship during turning.

Assuming that the actual drifting angle resulted from the manoeuvring simulation corresponds to the drifting angle in a drifting condition, in the next step we calculate the wake distribution on the propeller plane during drifting.

4.3 Estimating wake distribution using CFD during drifting

MHI uses CFD to estimate the wake distribution on the propeller plane during drifting. Previously, we used the wake distribution on the propeller plane measured from model tests in a drifting condition. At the earlier stage of design when the bearing was designed since the ship hull form was not yet fixed, the wake distribution was not available. We therefore used the results of model tests on similar ships to estimate the propeller shaft forces. We were however unable to cope with the differences in the changes in wake distribution on the propeller plane attributable to the differences between the ships. We only evaluated the changes in propeller shaft forces because of the differences in the propellers. To improve the reliability of bearing design, it is necessary to evaluate the changes in propeller shaft forces according to the actual ship hull form. By introducing CFD to estimate the wake distribution on the propeller plane, MHI has made this evaluation possible.

Figure 9 compares two wake distributions on the propeller plane, one measured in a model test and the other estimated by CFD. The CFD-estimated wake distribution on the propeller plane approximates well the lateral flow obtained from the model test. Based on these two types of wake distribution on the propeller plane, **Fig. 10** shows the tangential velocity Vt at the representative radius of 0.7R that are divided by the ship velocity U to make the non-dimentional values. The CFD estimation approximates well the changes in the tangential flow velocities with respect to each propeller rotational angle θ. The variance for one revolution of the propeller on Fig. 10 is calculated as 0.004. It is therefore fair to say that the two types agree well quantitatively.

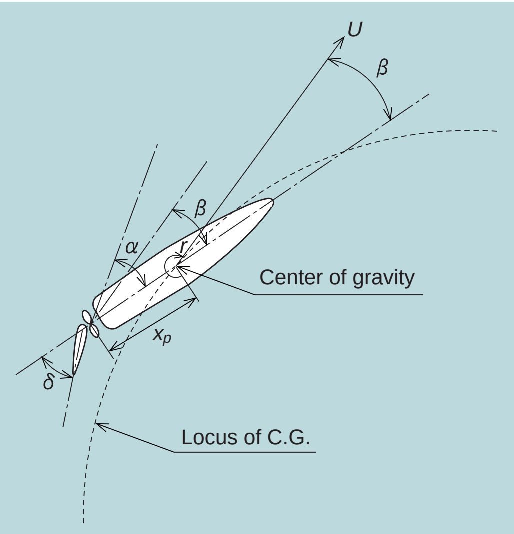

Fig. 8 Inflow angle into propeller
When turning at the rudder angle δ, the rate of turn r and the drifting angle β, water flows against the propeller plane at angle α.

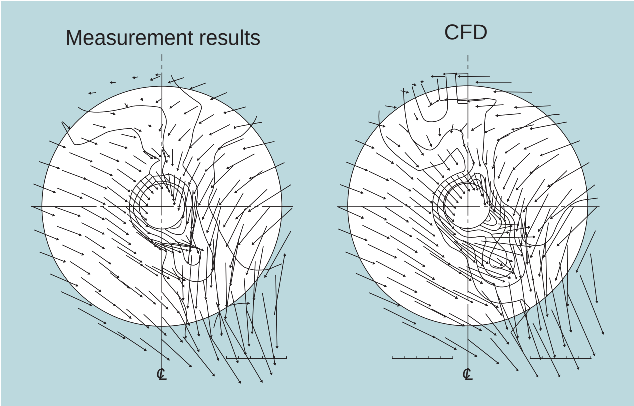

Fig. 9 Comparison of wake distribution on propeller plane
The wake distribution obtained by CFD approximates the lateral flow that appears on the results from the model test.

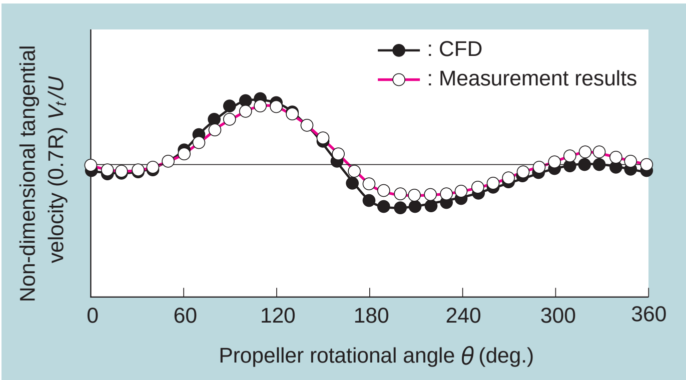

Fig. 10 Comparison of V_t/U at representative radius of 0.7R
The CFD-calculated results agree well with the model test results.

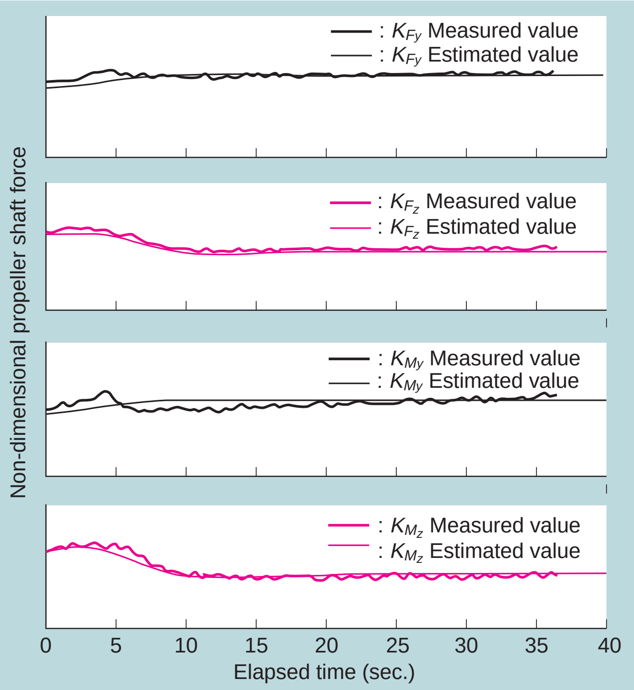

Fig. 11 Comparison of non-dimensional propeller shaft forces during turning
The values estimated by present method agree well with the model test results.

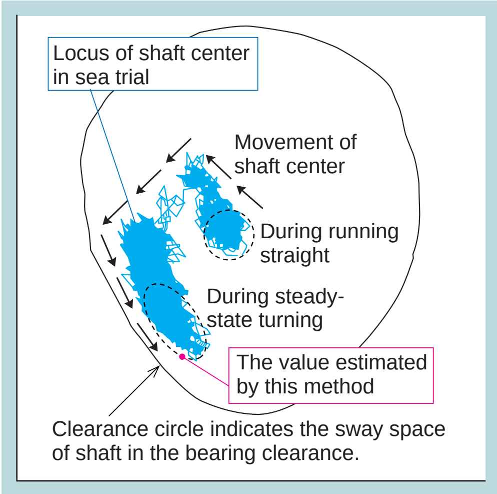

Fig. 12 Comparison of oil film thickness in stern tube bearing during turning
The distance between the clearance circle and the shaft center is the oil film thickness. The estimated values agree well with the results of the sea trial.

As we can see CFD is an effective tool which enables us to accurately estimate the wake distribution on a propeller plane during drifting.

Furthermore, the propeller shaft forces under two or more drifting conditions are calculated to obtain the relationship between the drifting angles and the propeller shaft forces. Then, the time-history of propeller shaft forces are obtained by interpolation with the time-history of actual drifting angles given by the manoeuvring simulation.

5. Application of bearing design method

MHI has applied this method to the bearing design of a container ship while conducting a model test and sea trial on an actual ship for verification. The model test provided us with the measured propeller shaft forces. Since it is difficult to measure the propeller shaft forces in a sea trial on an actual ship, we measured the oil film thickness to confirm the ability to form an oil film and to verify the adequacy of the estimated propeller shaft forces.

Figure 11 compares the estimated propeller shaft forces with those measured from the model test. The measured and estimated values changes similarly. As for steady-state turning, which is the most critical, the estimate also proves to be sufficiently accurate with respect to the absolute values. **Figure 12** compares the estimated oil film thickness in the stern tube bearing with that measured from the sea trial. The comparison shows that both values agree well.

As demonstrated above, this method enables us to accurately estimate propeller shaft forces and oil film thickness. It is an effective tool for designing stern tube bearings for ships.

6. Conclusion

Aided by CFD and manoeuvring simulation, we have established a method of estimating propeller shaft forces. It enables us to accurately estimate propeller shaft forces and the oil film thickness in a stern tube bearing. An accurate estimation enables us to design bearing profiles that prevent the uneaven contact and seizure of stern tube bearings. This contributes to improving the reliability of the bearings. We make efforts to offer ships with high reliability by applying this bearing design method to all MHI-built ships to prevent bearing damage.

References

(1) Yoshioka, M. et al., Strength and Materials of Propeller, Shafting, Bearing, The 5th Symposium on Marine Propellers (2005) p.201
(2) Chiba, N. et al., Measurement of Propeller Bearing Force, Mitsubishi Juko Giho Vol. 15 No. 3 (1978) p.1
(3) Ukon, Y. et al., Propeller Cavitation and Hydrodynamic Issues Induced by anCavitating Propeller, The 5th Symposium on Marine Propellers (2005) p.125
(4) Tetsuji Hoshino, Application of Quasi-Continuous Method to Unsteady Propeller Lifting Surface Problems, Journal of Marine Science and Technology Vol. 158 (1985) p.48


Ryota Kuroiwa

Akira Oshima

Tadasuke Nishioka

Tomohiro Tateishi

Kenji Ohyama

Takashi Ishijima